# MECHANICAL MODEL FOR FLEXURAL BEHAVIOUR OF SLAB-COLUMN CONNECTIONS UNDER SEISMICALLY INDUCED DEFORMATIONS

**Ioannis-Sokratis Drakatos, Aurelio Muttoni**

Structural Concrete Laboratory, Ecole Polytechnique Fédérale de Lausanne, Switzerland

**Katrin Beyer**

Earthquake Engineering and Structural Dynamics Laboratory, Ecole Polytechnique Fédérale de Lausanne, Switzerland

## Abstract

Reinforced concrete (RC) flat slabs supported on columns are one of the most widely used structural systems for office and industrial buildings. In regions of medium to high seismic risk RC walls are typically added as lateral force resisting system and to increase the lateral stiffness and strength. Although slab-column systems are not expected to contribute to the lateral resistance of the structure due to their low stiffness, the slab-column connection have to have the capacity to follow the seismically induced lateral displacements of the building while maintaining the capacity to transfer the vertical loads from the slab to the columns. Otherwise, brittle punching failure of the slab occurs and the deformation capacity of the entire building is limited by the deformation capacity of the connection. The present paper presents a model for predicting the flexural behaviour of slab-column connections without transverse reinforcement when subjected to earthquake-induced deformations, considering both the load and the deformation of the slab. The model is based on the Critical Shear Crack Theory (CSCT) and presents a rational approach for predicting the transferred moment-rotation relationship of slab-column connections as well as the contribution of all resistance-providing mechanisms respecting equilibrium principles in both local and global level. The model proved to be accurate enough when compared with tests (monotonic and cyclic) found in the literature.

**Keywords:** CSCT**,** Drift, Eccentricity, Flat slab, Moment transfer, Punching, Shear crack

## 1 Introduction

RC flat slabs supported on columns are one of the most popular structural systems for office and industrial buildings around the world, presenting several advantages (large open floor spaces, short construction times). Due to their low lateral stiffness, in seismic prone areas vertical spines (shear and/or core walls) are added to carry the largest portion of the horizontal loads generated during earthquakes and to increase the lateral stiffness and strength of the building. In this case, although the slab-column connections are not part of the lateral force resisting system, they must have the capacity to follow the seismically induced deformations of the building without losing their vertical load carrying capacity (Fig. 1a). Otherwise, brittle punching failure of the slab occurs and the deformation capacity of the connection determines the deformation capacity of the entire building.

The main shortcoming of proposed mechanical models for punching of RC slab-column connections under imposed deformations (Broms, 2009) as well as design approaches in codes of practice (ACI 318, 2008; Eurocode 2, 2004) is the empirical estimation of the contribution of the resistance-providing mechanisms of the theory of elasticity (eccentric shear force, bending and torsional moment). Approaches in codes feature additional shortcomings such as the assumption of linearly distributed shear stresses on the critical perimeter and lack of methods for calculating the moment transferred to the connection. Moreover, current codes (e.g. ACI 318, 2008) adopt

empirical models for estimating the seismic drift capacity of slab-column connections (Pan and Moehle, 1989) which application is limited to slab-column configurations against which they were calibrated.

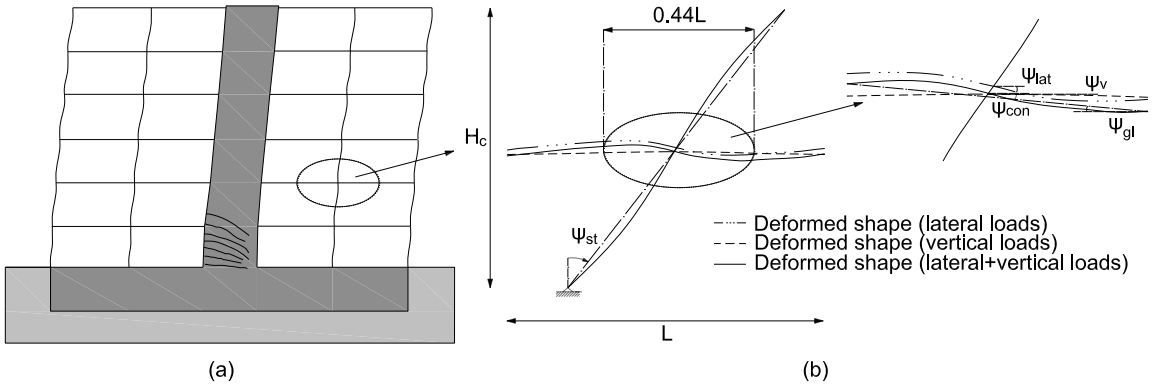


**Fig. 1** Seismically induced drift in slab-column connections: deformation state (a) at global level (reference building), and (b) local level (slab-column connection), where L is the span length and $H_c$ is the distance between mid-height of columns below and above the connection

To design and assess buildings with flat slabs and columns, the estimation of the moment-rotation relationship of slab-column connections and the rotation capacity are obligatory. Moreover, as punching is a brittle local failure due to excessive shear stresses in the proximity of the slab-column connection, the need for a relationship between local rotations and global interstorey drift $\psi_{st}$ becomes obvious (Fig. 1b). In addition the size effect, the gravity load effect, the influence of column size and the influence of the reinforcement ratio should be effectively captured by the moment-rotation relationship.

This paper presents a mechanical model for predicting the flexural behaviour of slab-column connections subjected to earthquake-induced drifts, considering both the load and the deformation of the slab. The model is based on the Critical Shear Crack Theory (CSCT) which has been employed successfully for predicting the flexural behaviour of slab-column connections for gravity induced loads considering both the load and the deformation ($\psi_v$ – see Fig. 1b) and which forms the basis of the punching shear equations of the FIB Model Code (2010). The extended model presents a rational approach for the relationship between transferred moment and rotation of slab-column connections due to the combination of lateral and vertical loads at local ($\psi_{con}$ – see Fig. 1b) and global ($\psi_{gl}$ – see Fig. 1b) level, respecting equilibrium principles as well as the contribution of all resistance-providing mechanisms. The model is also compared against tests found in the literature and is shown to yield good predictions of the moment – interstorey drift relationship.

## 2 Mechanical model for seismically induced drifts

The theoretical background of the proposed model is presented hereafter along with the modifications comparing to the CSCT. The load is assumed to be transferred to the column through an inclined compression strut. The presence of a critical shear crack that propagates along this strut reduces the shear strength of the connection (Muttoni, 2008). Therefore, the slab is divided into n sector elements and the region inside the shear crack. The difference comparing to the CSCT is the fact that the state of rotations is not the same for all the sector elements. Consequently torsional moments and moments due to eccentric shear force are introduced in the connection. The kinematic assumption and curvature distributions are demonstrated in Fig. 2. The equilibrium principles on the local level are illustrated in Fig. 3. The half of the slab where the transferred moment increases the deflection of the slab due to vertical loads is denoted as “negative slab half” (negative moment

due to seismic loading), whereas the other half where tension in the bottom reinforcement may appear is denoted as "positive slab half" (positive moment due to seismic loading).

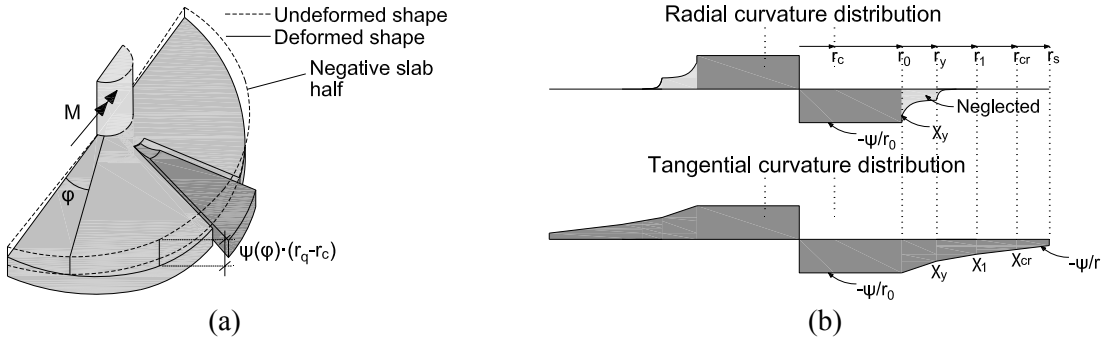


**Fig. 2** Proposed mechanical model: (a) kinematic assumption for the rotations of the sector elements (negative slab half), and (b) distribution of radial and tangential curvatures along the diameter of the isolated slab element (for upwards deflection of the positive slab half)

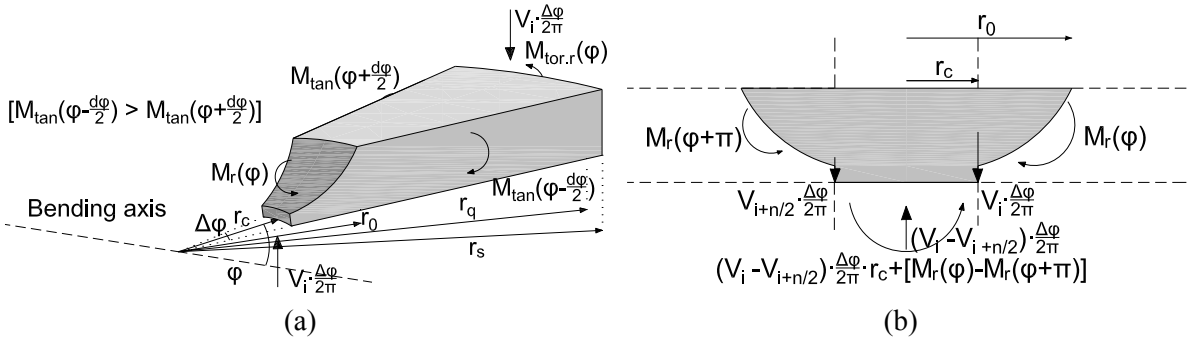


**Fig. 3** Internal forces acting on the slab region: (a) outside the shear crack (negative slab half), and (c) inside the shear crack

The additional assumptions that are made concerning the calculation of the moment-rotation relationship according to the proposed model are the following:

1) The rotation of the slab is assumed to follow a sinusoidal law with maximum value $\psi_{max}$ at 90° (tip of the negative slab half - Fig. 2a) and minimum value $\psi_{min}$ at 270° from the bending axis, as it is described in the following equation (angle φ measured from the bending axis):

$$\psi(\varphi) = \frac{\psi_{max} + \psi_{min}}{2} + \frac{\psi_{max} - \psi_{min}}{2} \cdot \sin\varphi \qquad (1)$$

2) No torsional moments are developed in the faces of the sector elements (rigid bodies).
3) The tangential moments are equal to the radial ones in the region inside the critical shear crack (Fig. 2c).
4) The radius $r_0$ of the critical shear crack is equal to the eccentricity e.
5) The quadrilinear moment-curvature diagram that is assumed for concentric punching (Muttoni, 2008) is also adopted as the envelope for the extended model.

The mathematical expressions are presented hereafter. $M_{tan(\varphi-\Delta\varphi/2)}$ and $M_{tan(\varphi+\Delta\varphi/2)}$ are the integrals of the tangential moments at the faces of each sector element (Fig. 2b). Subsequently these moments will be referred to as $M_{tan}^{-}$ and $M_{tan}^{+}$, respectively, and are determined directly as a function of the assumed rotation, using the following formula (quadrilinear moment-curvature relationship):

$$M_{tan}(\varphi)=\left(\begin{array}{c} m_R\left\langle r_y-r_0\right\rangle+EI_1\cdot\psi(\varphi)\cdot\left\langle \ln(r_1)-\ln(r_y)\right\rangle+ \\ +EI_1\cdot\chi_{TS}\cdot\left\langle r_1-r_y\right\rangle+m_{cr}\cdot\left\langle r_{cr}-r_1\right\rangle+EI_0\cdot\psi(\varphi)\cdot\left\langle \ln(r_s)-\ln(r_{cr})\right\rangle \end{array}\right) \quad (2)$$

where $EI_0$ and $EI_1$ are the stiffnesses before and after cracking, $m_{cr}$ and $m_R$ are the cracking moment and moment capacity respectively per unit width, $\chi_{TS}$ is the curvature due to the tension stiffening effect, and $r_0$, $r_y$, $r_1$, $r_{cr}$ and $r_s$ are the radii of the critical shear crack, of the yielded zone, of the zone in which cracking is stabilized, of the cracked zone and of the circular isolated slab element respectively. The operator $\langle x\rangle$ is x for $x \geq 0$ and 0 for $x < 0$. These parameters are the same as in CSCT (Muttoni, 2008). The only parameter that is updated for the case of seismically induced deformations is the radius $r_0$ of the critical shear crack (assumption 4) to take into account the fact that the shear force becomes less determinant as eccentricity increases. Therefore, the integral of the radial moment for a sector element at angle φ at $r = r_0$ is:

$$M_r(\varphi)=m_r(\varphi)\cdot r_0\cdot\Delta\varphi \quad (3)$$

where $m_r(\varphi)$ is the radial moment per unit width at $r = r_0$ as function of the radial curvature (Muttoni, 2008).

If $\varphi_i$ is the angle formed by the axis of bending and the bisector of the $i^{th}$ sector element, the shear force that can be carried from the compression strut of this sector element is derived by moment equilibrium in the tangential direction with respect to the centre of the column with radius $r_c$:

$$V_i\cdot\frac{\Delta\varphi}{2\pi}=\frac{1}{(r_q-r_c)}\cdot\{M_r(\varphi_i)+\left[M_{tan^-}(\varphi_i)+M_{tan^+}(\varphi_i)\right]\cdot\sin(\frac{\Delta\varphi}{2})\} \quad (4)$$

The total shear force acting on the connection for the load step k is:

$$V_k=\sum_{i=1}^{n}V_i\cdot\frac{\Delta\varphi}{2\pi} \quad (5)$$

The moment equilibrium in the radial direction gives the torsional moment that is carried by the connection for the $i^{th}$ sector element:

$$M_{tor.r}(\varphi_i)=\left[M_{tan^+}(\varphi_i)-M_{tan^-}(\varphi_i)\right]\cdot\cos(\frac{\Delta\varphi}{2}) \quad (6)$$

The different external loads acting on different sector elements provoke different moments for each load step k. The moment due to flexure (around the axis of the transferred moment) for the $i^{th}$ sector element is:

$$M_{flex.k}(\varphi_i)=V_i\cdot\frac{\Delta\varphi}{2\pi}(r_q-r_c)\cdot\sin(\varphi_i) \quad (7)$$

The component of the torsional moment $M_{tor.r}(\varphi_i)$ that is parallel to the transferred moment for the $i^{th}$ sector element is:

$$M_{tor.k}(\varphi_i)=[M_{tan^+}(\varphi_i)-M_{tan^-}(\varphi_i)]\cdot\cos(\frac{\Delta\varphi}{2})\cdot\cos(\varphi_i) \quad (8)$$

The difference of compression forces of the strut along the shear crack between anti-diametric sector elements provokes moment due to shear force difference and radial moment difference (Fig. 2d). The component that is parallel to the bending axis is denoted as $M_{ecc}$ and can be calculated using the following formula:

$$M_{ecc.k}(\varphi_i) = \left[ V_i \cdot \frac{\Delta\varphi}{2\pi} - V_{i+n/2} \cdot \frac{\Delta\varphi}{2\pi} \right] \cdot 2 \cdot r_c \cdot \sin(\varphi_i) + \left[ M_r(\varphi_i) - M_r(\varphi_{i+n/2}) \right] \cdot \sin(\varphi_i) \quad (9)$$

Therefore, the total moment acting on the connection (parallel to the transferred moment) for the load step k is:

$$M_k = \sum_{i=1}^{n} M_{flex.k}(\varphi_i) + \sum_{i=1}^{n} M_{tor.k}(\varphi_i) + \sum_{i=1}^{n/2} M_{ecc.k}(\varphi_i) \quad (10)$$

The total moment acting perpendicularly to the transferred moment is equal to zero ($M_{k,\perp} = 0$) and therefore global equilibrium is satisfied. The eccentricity calculated at load step k is:

$$e_k = M_k / V_k \quad (11)$$

To obtain the relationship characterizing the flexural behaviour an iterative procedure should be adopted. The maximum rotation $\psi_{max}$ is iterated so as to obtain the points that form the curve (denoted as load steps k) and the minimum rotation $\psi_{min}$ is calculated to satisfy local and global equilibrium. For constant eccentricity e the global equilibrium is satisfied when $e_k \approx e$ so the load-rotation curve is obtained and the radius $r_0$ of the shear crack is constant (assumption 4) throughout the iterative calculations. For constant shear force V acting to the connection the iterative process for each load step terminates when $V_k \approx V$ so the moment-rotation curve is obtained and the radius $r_0$ of the shear crack is adapted at each load step.

# 3 Comparison with experiments

The presented model is evaluated on the basis of experiments found in the literature, conducted either by monotonic application of loads (e.g. Krüger, 1999) or by quasi-static cyclic moment introduction (e.g. Pan and Moehle, 1989). The state of column deformations that inherently influences the rigid body rotations in the region inside the shear crack was taken into account depending on the test setup configuration.

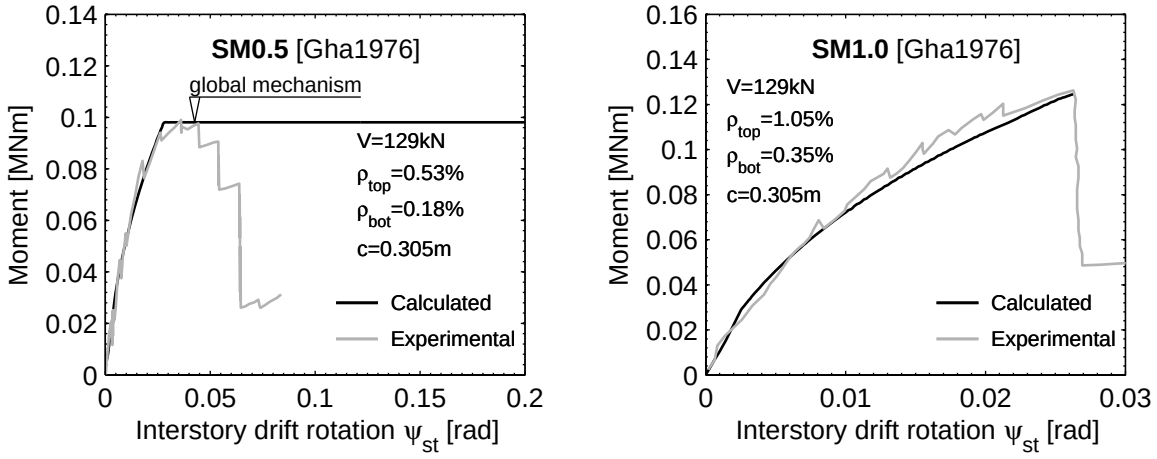


(a) (b)

**Fig. 4** Influence of reinforcement ratio for monotonic tests under constant vertical load (Ghali et al, 1976): (a) 0.5%, and (b) 1.0%

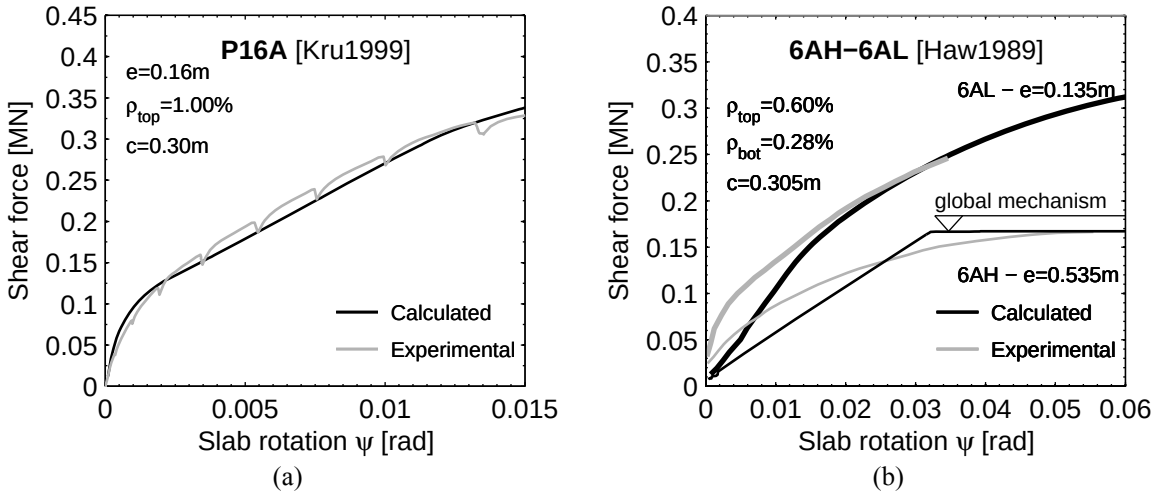


**Fig. 5** Comparison with monotonic tests under constant eccentricity: (a) Krüger (1999), and (b) Hawkins et al. (1989)

The model predictions show satisfactory agreement with the experimentally observed behaviour of slab-column connections subjected to monotonically increasing transferred moments, either under constant vertical load (Ghali et al., 1976), or under constant eccentricity (Krüger, 1999; Hawkins et al., 1989). The influence of the reinforcement ratio is effectively captured (Fig. 4). It should be noted that the iterative procedure ends either when the slab reaches the global mechanism (Fig. 4a) or when the radius of the critical shear crack $r_0$ exceeds the dimensions of the tested specimen (border effect - Fig. 4b). For the experiments carried out by Hawkins et al. (1989) an underestimation of the initial stiffness is observed (Fig. 5b). However, the softening of the flexural response under the effect of increasing eccentricity due to the formation of a wider critical shear crack in the negative slab half (Tassinari, 2011) is captured by the proposed model.

Concerning the cyclic behaviour, the presented model adopts a monotonic moment-curvature relationship for both directions of loading. Therefore, the influence of degradation due to cyclic loading to the moment-rotation relationship is neglected.

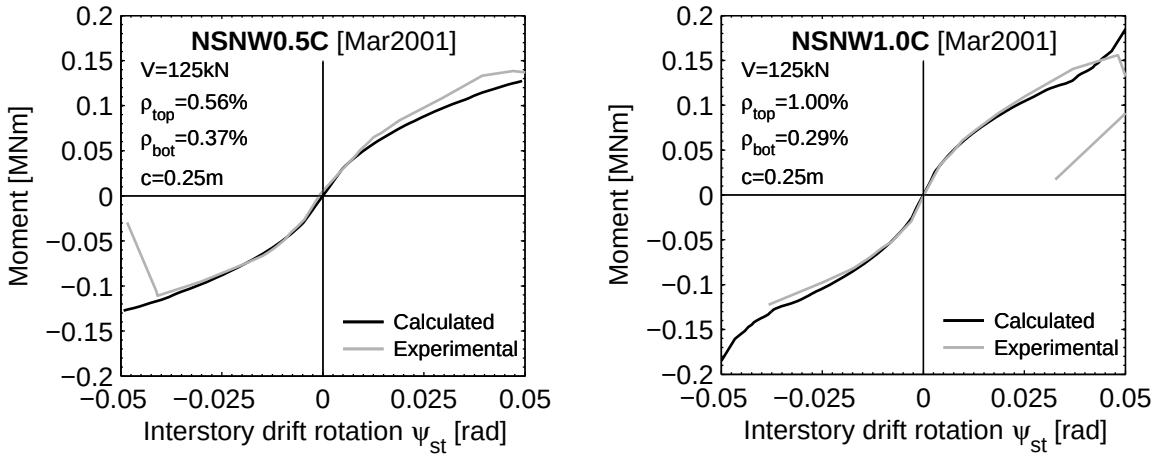


**Fig. 6** Influence of reinforcement ratio for cyclic tests (Marzouk et al., 2001)

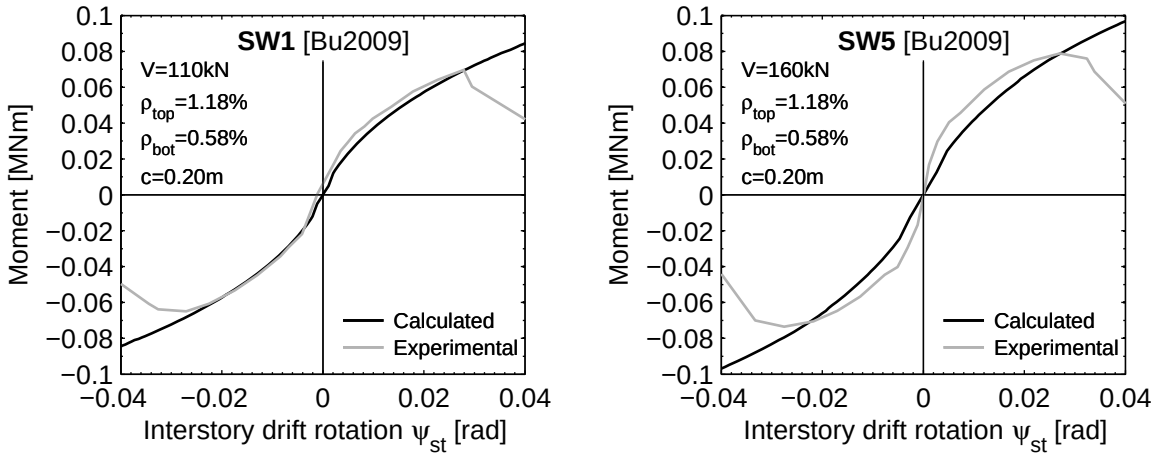


(a)

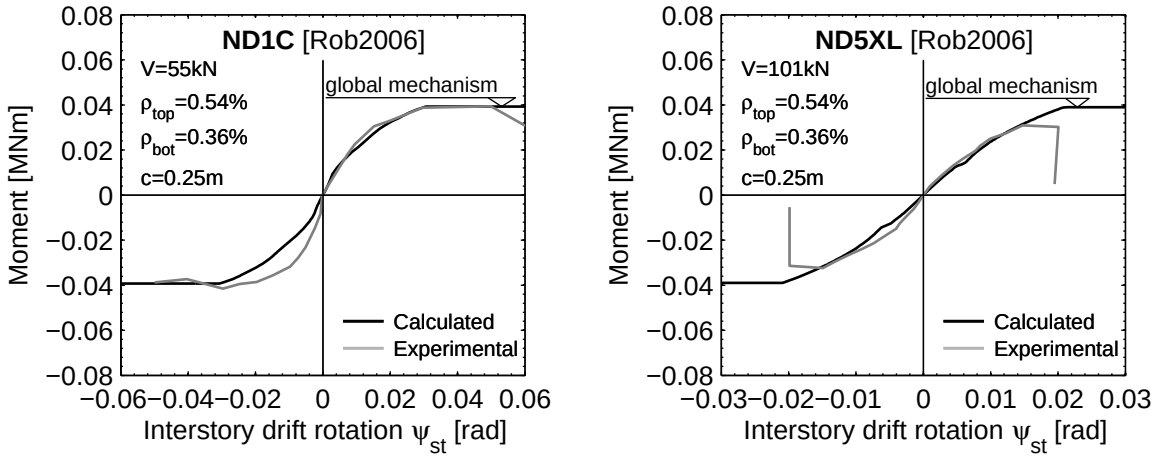


(b)

**Fig. 7** Gravity load effect for cyclic tests: (a) Bu and Polak (2009), and (b) Robertson and Johnson (2006)

The model predicts accurately enough the moment-rotation relationship also for the cyclic tests found in the literature. It is capable to accurately predict the effect of reinforcement ratio also for cyclic tests (Marzouk et al., 2001) as well as the gravity load effect (Bu and Polak, 1989; Robertson and Johnson, 2006). Moreover, as can be seen from Fig. 6 and Fig. 7, the tested specimens did not exhibit any significant sign of degradation due to cyclic loading. Therefore the aforementioned assumption seems to be realistic.

# 4 Conclusions and Outlook

A mechanical model to describe the flexural behaviour of RC slab-column connections under seismically induced deformations is presented. The model is based on the CSCT and can effectively uncouple the contribution of the various resisting mechanisms (flexure, eccentric shear force and torsion) when a slab-column connection is subjected to earthquake-induced deformations.

The model predicts accurately enough the moment-rotation relationship for tests found in the literature, conducted either by monotonically or cyclically increasing loading. The presented model can capture the influence of the reinforcement ratio and the effect of eccentricity for monotonic tests. Moreover, the gravity load effect as well as the influence of the reinforcement ratio are captured for cyclic tests.

When comparing experimental and predicted curves no significant sign of degradation due to cyclic loading appeared to exist for moment-rotation relationships. The results of an ongoing experimental campaign will provide more insight into the behaviour of slab-column connections when subjected to cyclic loading by comparing it to the behavior of slab-column connections subjected to monotonically increasing loading. Moreover, it is anticipated that these new tests will offer a better understanding of the contribution of resistance-providing mechanisms and of the parameters that are influencing the failure criterion. Other aspects, such as the column size effect, will also be investigated.

## Acknowledgements

The present investigation, funded by the Federation of the Swiss Cement Industry (CemSuisse), is gratefully acknowledged.

## References

ACI (2008), Building code requirements for structural concrete (ACI 318-08) and commentary (ACI 318R-08), American Concrete Institute, Farmington Hills, USA.

Broms, C.E. (2009), Design method for imposed rotations of interior slab-column connections, ACI Structural Journal, Vol. 106, No. 6, pp. 636-645.

Bu, W.; Polak, M.A. (2009), Seismic retrofit of reinforced concrete slab-column connections using shear bolts, ACI Structural Journal, Vol. 106, No. 4, pp. 514-522.

Eurocode 2 (2004), Design of concrete structures – Part 1-1: General rules and rules for buildings, CEN, EN 1992-1-1, Bruxelles, Belgium.

*fib* Bulletin 56 (2010), Model code 2010 – First complete draft. Fédération internationale du béton (*fib*), Lausanne, Switzerland.

Ghali, A.; Elmasri, M.Z.; Dilger, W. (1976), Punching of flat plates under static and dynamic horizontal forces, ACI Structural Journal, Vol. 73, No. 10, pp. 566-572.

Hawkins, N.M.; Bao, A.; Yamazaki, J. (1989), Moment transfer from concrete slabs to columns, ACI Structural Journal, Vol. 86, No. 6, pp. 705-716.

Krüger, G. (1999), Résistance au poinçonnement excentré des planchers-dalles, Ph.D. thesis, Ecole Polytechnique Fédérale de Lausanne, Switzerland.

Marzouk, H.; Osman, M.; Hussein, A. (2001), Cyclic loading of high-strength lightweight concrete slabs, ACI Structural Journal, Vol. 98, No. 2, pp. 207-214.

Muttoni, A. (2008), Punching shear strength of reinforced concrete slabs without transverse reinforcement, ACI Structural Journal, Vol. 105, No. 4, pp. 440-450.

Pan, A.; Moehle, J.P. (1989), Lateral displacement ductility of reinforced concrete flat plates, ACI Structural Journal, Vol. 86, No. 3, pp. 250-258.

Robertson, I.; Johnson, G. (2006), Cyclic lateral loading of nonductile slab-column connections, ACI Structural Journal, Vol. 103, No. 3, pp. 356-364.

Tassinari, L. (2011), Poinçonnement non symétrique des dalles en béton armé, Ph.D. thesis, Ecole Polytechnique Fédérale de Lausanne, Switzerland.